Spray pyrolysis growth and characterization of $Cd_{1-x}Zn_xS$ thin films

P. M. PARAMESHWARI, K. GOPALAKRISHNA NAIK*
Department of Physics, Mangalore University, Mangalagangotri - 574199, India

$Cd_{1-x}Zn_xS$ thin films with zinc content x = 0.0, 0.2, 0.4, 0.6, 0.8, and 1.0 were deposited by the spray pyrolysis method using $CdCl_2$ (0.15 M), $ZnCl_2$ (0.15 M) and H_2NCSNH_2 (0.15 M) solutions on glass substrates at 400°C. The prepared $Cd_{1-x}Zn_xS$ films were characterized with XRD, FESEM, EDS and UV-Visible spectroscopic technique for structural, morphological, elemental composition, and optical study. X-ray diffraction results showed that the $Cd_{1-x}Zn_xS$ thin films formed were polycrystalline with hexagonal structures at low Zn content. As the Zn content was increased, the XRD peak position shift towards higher 2θ and for Zn content x~0.8 the crystal structure transforms into cubic. The formation of $Cd_{1-x}Zn_xS$ alloy was confirmed by elemental analysis by EDS and optical absorption spectroscopy. With increase in Zn content in the spray solutions, the grown $Cd_{1-x}Zn_xS$ thin films show proportionate in increase in bandgap energy. The transmittance of $Cd_{1-x}Zn_xS$ thin films was increased with increase of Zn content and it was above 80 % in the visible region.
PACS: 68.55.-a; 78.20.-e

(Received January 20, 2014; accepted November 13, 2014)

Keywords: Spray pyrolysis, $Cd_{1-x}Zn_xS$ thin films, Lattice parameter, Energy band gap

1. Introduction

The wide band gap cadmium zinc sulfide ($Cd_{1-x}Zn_xS$) semiconductor material has been extensively investigated for their applications in various solid state devices [1, 2]. In solar cells, the replacement of the widely used CdS window layer with $Cd_{1-x}Zn_xS$ leads to decrease in window absorption losses resulting in an increase in the short circuit current and open circuit voltage in solar cell [3, 4]. In recent year's great attention has been given to the investigation of the properties of $Cd_{1-x}Zn_xS$ thin films grown by various methods in order to improve the performance of these thin films [3, 5]. The thin film deposition techniques such as spray pyrolysis [2, 6, 7], molecular beam epitaxy [8], SILAR [9], vacuum evaporation [5], chemical bath deposition [10], and solution growth [11, 12] have been used to grow $Cd_{1-x}Zn_xS$ thin films. In this study $Cd_{1-x}Zn_xS$ thin films were deposited with Zn content x = 0.0, 0.2, 0.4, 0.6, 0.8, and 1.0 by spray pyrolysis technique. The effects of Zn content on the properties of $Cd_{1-x}Zn_xS$ thin films were investigated.

2. Experimental

$Cd_{1-x}Zn_xS$ thin films were deposited on glass substrates by spray pyrolysis technique. Aqueous solutions of 0.15M $CdCl_2$, 0.15M $ZnCl_2$, 0.15M $(NH_2)_2CS$ were used as a source of cadmium, zinc and sulphur, respectively. The precursor solutions were mixed in appropriate quantities, as given in the Table 1, in order to get required composition, and stirred for half an hour using a magnetic stirrer. The thin films were obtained by spraying these solutions on the glass substrates kept at temperature of about 400^0C at a spray rate of 10 ml per minute. The grown films were allowed to cool naturally to room temperature.

Table 1. Spray solution compositions.

Composition of $Cd_{(1-x)}Zn_xS$ film x	$CdCl_2$ (0.15 M)	$ZnCl_2$(0.15M)	$(NH_2)_2CS$ (0.15M)
0.0	10 ml	-	10 ml
0.2	8 ml	2 ml	10 ml
0.4	6 ml	4 ml	10 ml
0.6	4 ml	6 ml	10 ml
0.8	2 ml	8 ml	10 ml
1.0	-	10 ml	10 ml

The structural properties of the films were characterized by X-ray powder diffractometer (Rigaku miniflex 600) using Cu Kα radiation (λ = 1.54178 Å). Full width at half maximum (FWHM) and 2θ values of the peaks was used to calculate the crystallite size.

Surface morphology of the films was studied using FESEM (Hitachi SU6600). Chemical composition of the films was obtained by energy dispersive X-ray spectroscopy (EDS). Thickness of the films was measured by an Ellipsometer (Holmarc opto mechatronics) using DPSS laser (532 nm) beam. Optical absorption and transmittance of the films were studied using Shimadzu 1800 UV-Vis spectrophotometer.

3. Results and discussion

3.1 Structural properties of $Cd_{1-x}Zn_xS$ thin films

The structural properties of spray deposited $Cd_{1-x}Zn_xS$ thin films were investigated by X-ray powder diffraction (XRD) using CuK_α radiation. Fig. 1 shows the X-ray diffraction patterns of the $Cd_{1-x}Zn_xS$ thin films deposited on glass substrates.

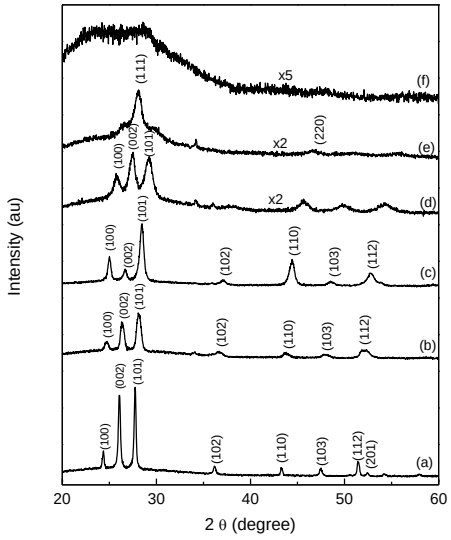

Fig. 1 XRD patterns of thin films of (a) CdS, (b) $Cd_{0.8}Zn_{0.2}S$, (c) $Cd_{0.6}Zn_{0.4}S$, (d) $Cd_{0.4}Zn_{0.6}S$, (e) $Cd_{0.2}Zn_{0.8}S$, and (f) ZnS.

The XRD patterns indicate the polycrystalline nature of the grown films. The XRD spectra of the films are indexed based on the JCPDS card No. 00-041-1049 (for CdS), 00-049-1302 (for hexagonal $Cd_{1-x}Zn_xS$) and 01-079-6259 (for cubic $Cd_{1-x}Zn_xS$). At low Zn content, the XRD results show that the $Cd_{1-x}Zn_xS$ thin films were polycrystalline with hexagonal structures with the peaks corresponding to (100), (002), (101), (102), (110), (103), (112) reflections in the 2θ range from 20^0 to 60^o. As the Zn content was increased, the XRD peaks slightly shift towards higher 2θ values. The progressive shift of the XRD patterns with increasing Zn content indicates that the thin films obtained were the homogeneous alloys of $Cd_{1-x}Zn_xS$ [13, 14]. The XRD spectra of $Cd_{1-x}Zn_xS$ corresponding to x ~ 0.6 looks different from that of the XRD spectra corresponding to low Zn content and it matches with the spectra corresponding to $Cd_{1.7}$ $Zn_{0.3}$ S_2 (JCPDS No: 01-079-3169) [15]. At Zn content x~0.8 the structure transforms from hexagonal to cubic with dominant (111) peak. As indicated by the XRD pattern, the grown ZnS thin film shows almost an amorphous structure. Lattice constants 'a' and 'c' of $Cd_{1-x}Zn_xS$ (x= 0 to 0.6) thin films and the lattice constant 'a' of $Cd_{1-x}Zn_xS$ (x= 0.8) thin film was calculated respectively from the diffraction angles of (100) and (002) planes corresponding to that of hexagonal phase and the diffraction angle of (111) planes corresponding to that of cubic phase, using the relationship between miller indices (h k l), lattice constants (a, b, c) and the interplanar distance (d) [16, 17].

It was observed that the lattice constant gradually decreases as Zn content increases for hexagonal structure; this is consistent with the smaller size of the zinc atom as compared to cadmium atom. The lattice parameters obtained from XRD analysis are given in the Table 2. The crystallite size was calculated using the angle and FWHM of the highest intensity peak by applying Scherer formula [18, 19] and thus obtained crystallite size values are listed in the Table 2. The crystallite size decreases with increase in the Zn content in the films.

Table 2. Crystallite size and lattice parameter variations with composition of the $Cd_{1-x}Zn_x$ S thin films.

Zn content in solution (x)	Crystallite size (nm)	Lattice parameters		
		a (Å)	c (Å)	c/a
0.0	38.52	4.1772	6.7723	1.6213
0.2	15.13	4.1573	6.7637	1.6269
0.4	15.16	4.1100	6.6767	1.6245
0.6	10.84	3.9729	6.4901	1.6336
0.8	4.17	5.4897		
1.0	1.15			

3.2 Surface morphology and elemental composition

Fig. 2(a) – 2 (f) shows the FESEM images of surface of the CdZnS thin films on glass substrates with different Zn concentration. The growth of the films was found to be uniform and dense across the substrate surface. There was a noticeable difference in the surface morphology of the films with different Zn content.

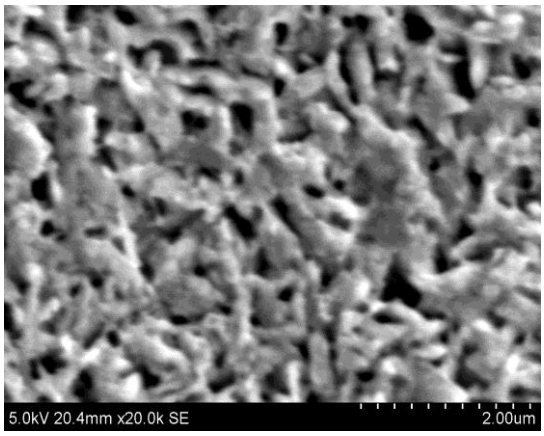

Fig. 2 (a) FESEM images of CdS.

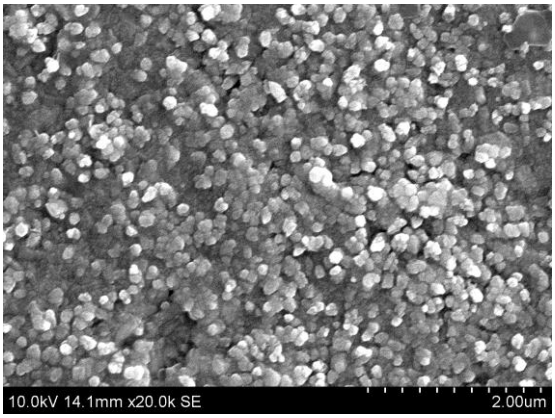

Fig. 2 (b) FESSEM image of $Cd_{0.8}Zn_{0.2}S$.

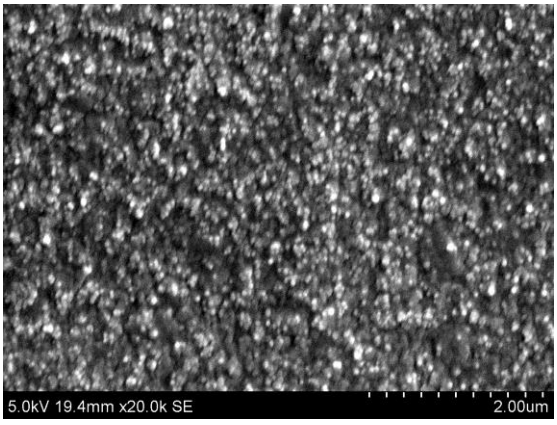

Fig. 2 (c) FESSEM image of $Cd_{0.6}Zn_{0.4}S$.

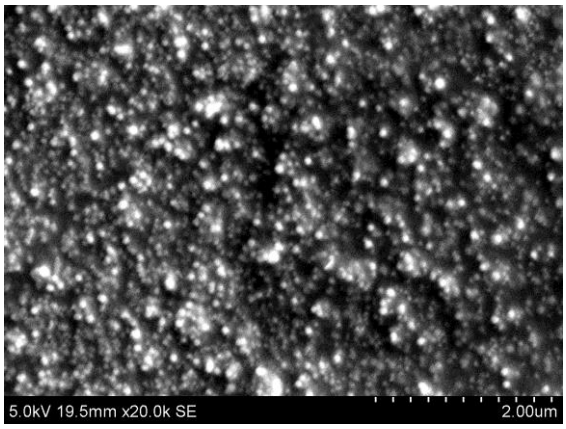

Fig. 2. (d) FESSEM image of $Cd_{0.4}Zn_{0.6}S$.

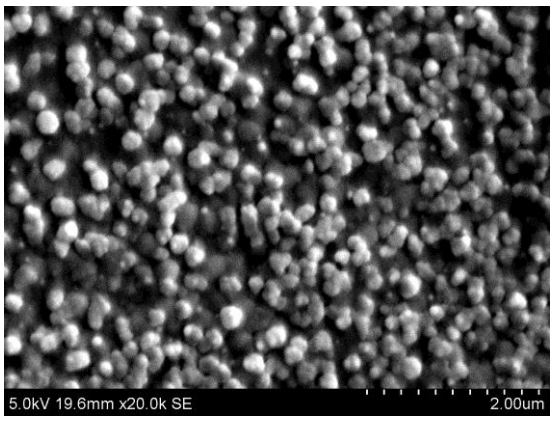

Fig. 2 (e) FESEM image of $Cd_{0.2}Zn_{0.8}S$.

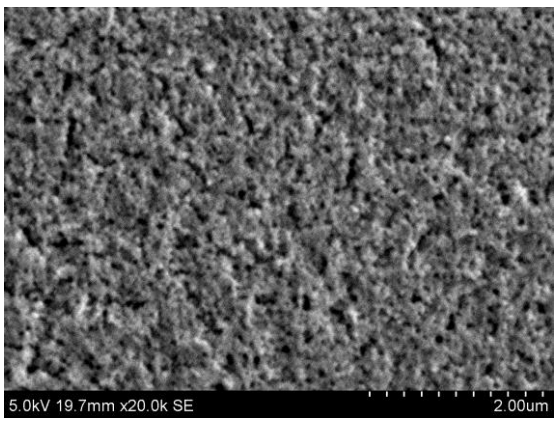

Fig. 2 (f) FESEM image of ZnS.

Uniformly distributed granules are observed in the films with the composition $Cd_{0.8}Zn_{0.2}S$ and $Cd_{0.2}Zn_{0.8}S$. The films with composition $Cd_{0.6}Zn_{0.4}S$ and $Cd_{0.4}Zn_{0.6}S$ appears to be extremely dense, whereas CdS and ZnS films are porous in nature. Elemental composition in the films was obtained from the EDS analysis. The obtained compositions were found to be almost same as that in the initial solutions, shown in Table 3. The zinc content in the films was found to be increase with increase in zinc content in the spray solution.

Table 3. Elemental composition of the $Cd_{1-x}Zn_x$ S thin films estimated from EDS.

Composition, x in solution	Cadmium (%)	Zinc (%)	Sulphur (%)	Composition, x in film
0.0	45.04	-	54.96	0.0
0.2	41.12	11.63	47.25	0.22
0.4	36.63	18.58	44.79	0.33
0.6	21.02	33.03	45.96	0.61
0.8	11.39	44.43	44.19	0.79
1.0	-	55.61	44.39	1.0

3.3. Optical properties of $Cd_{1-x}Zn_xS$ thin films

The optical absorption spectra of $Cd_{1-x}Zn_xS$ thin films were recorded in the wavelength range of 300 - 900 nm using shimadzu 1800 spectrophotometer. The absorption spectra are as shown in the Fig. 3 (a). The fundamental absorption edge of the as-deposited $Cd_{1-x}Zn_xS$ thin films showed a blue shift with an increase in Zn content. Thickness of the film was measured using a Holmarc Opto-Mechatronics (P) Ltd. India (www.holmarc.com) single wavelength ellipsometer (model no: HO-TCE-01). The ellipsometer consists of a laser (532 nm, randomly polarized), a polarizer (Glan-Thompson Prism) and a quarter wave plate which provide a state of polarization which can be varied from linearly polarized light to elliptically polarized light to circularly polarized light by varying the angle of the polarizer. For the measurement of the thin film thickness, the polarized laser beam is made to incident on the thin film sample at an angle of incidence 70^0. The reflected beam is analyzed with the analyzer (Glan-Thompson Prism) and the detector. The angles of the polarizer and analyzer were changed until a minimal signal (or null condition) is detected. The corresponding angles of the polarizer and analyzer were measured. Software provided along with the instrument is used to calculate the thickness of the films. All the films in this study have thickness of ~ 190 nm. By knowing the absorbance and thickness, absorption coefficient of the films can be calculated from the Beer-Lambert equation [20].

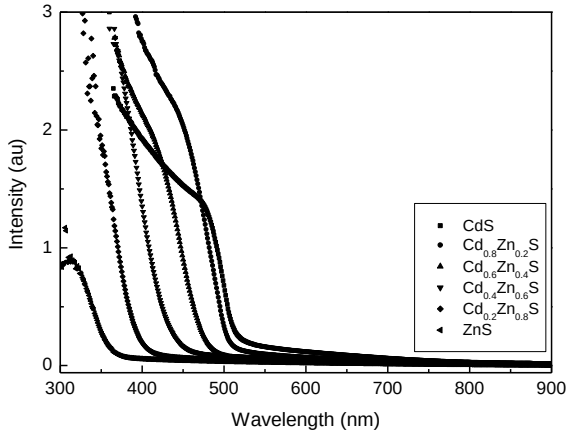

Fig. 3 (a). Plot of UV-vis absorption spectra of the Cd $_{1-x}$ Zn $_x$ S thin films.

The band gap E_g of the $Cd_{1-x}Zn_xS$ thin films were obtained from the optical absorption spectra using the Tauc relationship [2]

$$\alpha h\upsilon = C(h\upsilon - E_g)^n \quad (1)$$

where C is a constant, hυ is the energy of light and the exponent 'n' characterizes the nature of band transition, n = ½ for direct band gap semiconductor material. The graph of $(\alpha h\upsilon)^2$ versus hυ are plotted as shown in the Fig. 3 (b) The linear nature of the graph at the absorption edge confirmed that as deposited films are semiconductor with direct band gap [2]. The extrapolation of linear region of the curve to the energy axis gives the band gap values and these are listed in the Table 4. The band gap of $Cd_{1-x}Zn_xS$ thin films was calculated in range x from 0 to 1 using the quadratic relation [21]

$$E_{g\ (Cd_{1-x}Zn_xS)} = x\,E_{g\ ZnS} + (1-x)\,E_{g\ CdS} - bx(1-x) \quad (2)$$

where b is the bowing parameter. The value of b was obtained by fitting Eq. (2) with the experimental data using the experimentally obtained values of E_{gCdS} (2.46 eV) and E_{gZnS} (3.576 eV) and it was found to be 0.63. The variation of band gap of the $Cd_{1-x}Zn_xS$ thin films with Zn content along the bandgap calculated using Eq. (2) is shown in Fig. 4.

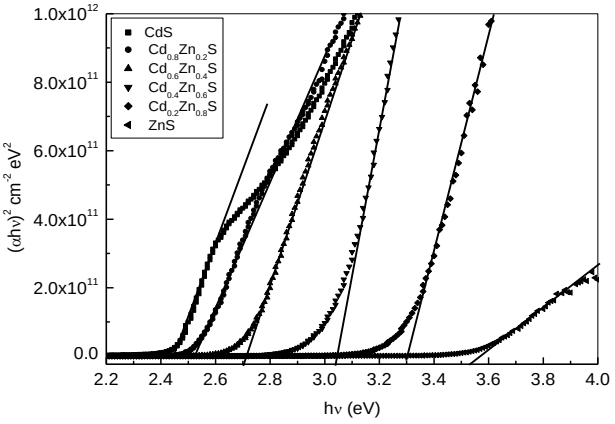

Fig. 3(b) Plot of $(\alpha h\nu)^2$ vs. hν for the $Cd_{1-x}Zn_xS$ thin film.

Table 4. Band gap variation with composition.

Composition , x in solution	Energy gap E_g (eV) from Uv-vis absorption spectra
0.0	2.46
0.2	2.582
0.4	2.755
0.6	2.978
0.8	3.252
1.0	3.576

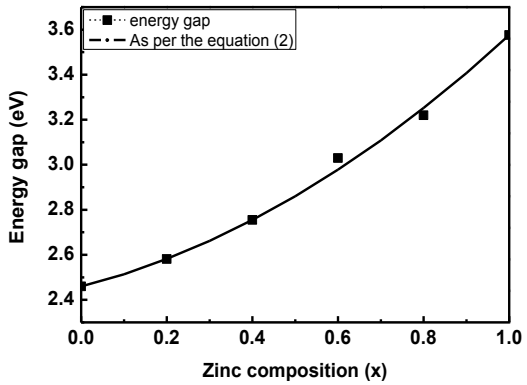

Fig. 4. The variation of band gap of the $Cd_{1-x}Zn_xS$ thin films with Zn content.

Transmittance spectra of the films were recorded in the wavelength range of 300 nm – 1000 nm. Transmittance of the films increases with increase in zinc content and it was found to be above 80 %, as shown Fig. 5.

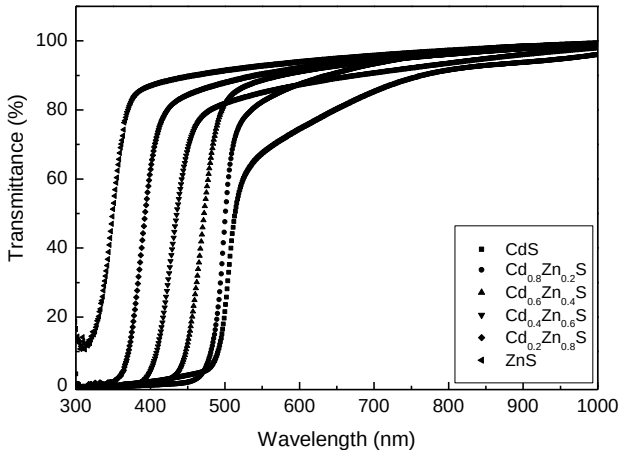

Fig. 5. Plot UV-vis transmittance spectra of the $Cd_{1-x}Zn_xS$ thin films.

4. Conclusions

$Cd_{1-x}Zn_xS$ thin films were successfully deposited using an aqueous solutions of $CdCl_2$, $ZnCl_2$ and $(NH_2)_2CS$ by spray pyrolysis technique. XRD studies reveal that the films are single phase, polycrystalline in nature. EDX analysis confirmed the increase in zinc content in the films with the increase of zinc composition in the spray solution. Variation in the surface morphology with the elemental composition can be clearly seen from SEM images of as deposited films. The fundamental absorption edge of as-deposited $Cd_{1-x}Zn_xS$ thin films, show a blue shift with an increase in the zinc ion content. Energy gap of $Cd_{1-x}Zn_xS$ films increased from 2.4 eV to 3.57 eV as 'x' is increased from 0.0 to 1.0. Transmittance of the films increased with increase of zinc content in the film. Relatively high transmission above fundamental absorption edge of the films indicate that these films are well suited as a window layer in the thin film heterojunction solar cells with CdTe, CIGS, and $CuInS_2$ as an absorber layer.

Acknowledgements

The authors acknowledge the financial support of DST-PURSE Project (MU/CHEM/PURSE PIG/2012) of the Mangalore University. The authors acknowledge INUP, Center for Nanoscience, IISc, Bangalore for providing characterization facility. Authors gratefully acknowledge the help and support of staff and research scholars of Department of Physics, and Microtron centre - Department of Physics, Mangalore University during the course of this work.

References

[1] S. Stolyarova, M. Weinstein, Y. Nemirovsky, J. Cryst. Growth **310,** 1674 (2008).
[2] M. C. Baykul, N. Orhan, Thin Solid Films **518**, 1925 (2010).
[3] W. Xia, J. A. Welt, Hao Lin, H. N. Wu, Meng H. Ho, Ching W. And Tang, Sol. Energy Mater. Sol.Cells **94**, 2113 (2010).
[4] I. O. Oladegi, L. Chow, C. S. Ferekides, V. Viswanathan, Z. Zhao, Sol. Energy Mater. Sol. Cells **61**, 203 (2000).
[5] J. Lee, W. Song, J. Yi, K. Yang, W. Hanc, J. Hwang, Thin Solid Films **431 –432**, 349 (2003).
[6] T. A. Chynoweth, R. H. Bube, J. Appl. Phys. **51**, 1844 (1980).
[7] R. S. Feigelson, A. N'Diaye, S. Y. Yin, R. H. Bube, J. Appl. Phys. **48**, 3162 (1977).
[8] T. Karasawa, K. Ohkawa, T. Mitsuya, J. Appl. Phys. **69**, 3226 (1991).
[9] M. P. Valkonen), S. Lindroos, M. Leskela, Appl. Surf. Sci. **134**, 283 (1998).
[10] R. Mariappan, M. Ragavendar, V. Ponnuswamy, Journal of Alloys and Compounds, **509**, 7337 (2011).
[11] Y. F. Nicolau, J. C. Menard, J. Cryst. Growth **92**, 128 (1988).
[12] G. K. Padam, G. L. Malhotra, S. U. M. Rao, J. Appl.

Phys. **63,** 770 (1988).
[13] C. Xing, Y. Z., Zhang, W. Yan, L. Guo, International Journal of Hydrogen Energy **31**, 2018 (2006).
[14] S. Jana, R. Maity, S. Das, M. K. Mitra, K. K. Chattopadhyay, Physica E **39,** 109 (2007).
[15] B. J. Skinner, P. M. Bethke, Am. Mineral **46**, 1382 (1961).
[16] B. D. Cullity, Elements of X-ray diffraction, Page No. 88, Addition-Wesley Publishing Company, Inc. (1956).
[17] A. R.Verma, O. N. Srivastava, Crystallography Applied to Solid State Physics 2nd edn, Page No. 80, New Age International (P) Limited, Publishers (1991).
[18] S. Kumar, P. Sharma, V. Sharma, J. Appl. Phys. **111**, 043519 (2012).
[19] B. D. Cullity, Elements of X-ray diffraction, Page No. 99, Addition-Wesley Publishing Company, Inc. (1956).
[20] Juan Chu , Zhengguo Jin, Shu Cai, Jingxia Yang , Zhanglian Hong, Thin Solid Films **520,** 1826 (2012).
[21] H. Hill, J. Phys. **C: 7**, **521** (1974).

*Corresponding author: gopal_mng@yahoo.com